Journal of Molecular Spectroscopy 284-285 (2013) 21–28

Contents lists available at SciVerse ScienceDirect

Journal of Molecular Spectroscopy

journal homepage: www.elsevier.com/locate/jms

The pure rotational spectrum of glycolaldehyde isotopologues observed in natural abundance

P. Brandon Carroll [a], Brett A. McGuire [a], Daniel P. Zaleski [b], Justin L. Neill [b], Brooks H. Pate [b,*], Susanna L. Widicus Weaver [a,*]

[a] Department of Chemistry, Emory University, 1515 Dickey Drive Atlanta, GA 30322, USA
[b] Department of Chemistry, University of Virginia, McCormick Rd., Charlottesville, VA 22904, USA

ARTICLE INFO

Article history:
Received 14 December 2012
In revised form 21 January 2013
Available online 8 February 2013

Keywords:
Glycolaldehyde
Rotational spectroscopy
Chirped-pulse spectroscopy
Broadband spectroscopy
Microwave spectroscopy

ABSTRACT

The pure rotational spectrum of glycolaldehyde has been recorded from 6.5–20 GHz and 25–40 GHz in two pulsed-jet chirped pulse Fourier transform microwave spectrometers. The high phase stability of the spectrometers enables deep signal integration, allowing transitions from the ^{13}C-substituted, ^{18}O-substituted, and deuterium-substituted isotopologues to be observed in natural abundance. Transitions from $HCOCH_2{}^{18}OH$ are reported for the first time. Additional transitions from the ^{13}C-substituted, deuterium-substituted, and $HC^{18}OCH_2OH$ isotopologues, as well as previously unobserved weak lines from the main isotopologue, have been observed. Transitions from all isotopologues are used with previously reported transitions to refine the spectroscopic parameters for each isotopologue. A Kraitchman analysis was performed using the experimental rotational constants to determine the molecular structure of glycolaldehyde.

© 2013 Elsevier Inc. All rights reserved.

1. Introduction

Glycolaldehyde ($HCOCH_2OH$) is the simplest α-hydroxy aldehyde, and as a sugar-related species is important in prebiotic chemical pathways. Glycolaldehyde is one of a set of complex organic molecules (COMs) detected in the interstellar medium (ISM), and is one of the few members of the $C_nH_{2n}O_n$ family to be detected thus far. Given its importance as a prebiotic molecule and the level of its chemical complexity compared to other COMs, detection of glycolaldehyde in an astronomical source and determination of its physical properties can provide important insight into the complex chemistry of the source. Glycolaldehyde has been detected in three interstellar sources, Sgr B2(N) [1–3], G31.41+0.31 [4], and IRAS 16293-2422 [5], and tentatively detected in G24.78+0.08 [6], through observations of its pure rotational spectral lines at microwave, millimeter, and submillimeter wavelengths. New submillimeter observatories such as the Atacama Large Millimeter Array (ALMA), the Stratospheric Observatory for Infrared Astronomy (SOFIA), and the Herschel Space Observatory (HSO) are providing observations with unprecedented spectral sensitivity and spatial resolution. The increased sensitivity of these instruments over existing ground-based observatories will enable the detection of glycoladehyde and other COMs in many additional sources. Indeed, the recent detection of glycolaldehyde lines in IRAS 16293-2422 was from an ALMA science verification dataset [5].

Reported isotopic ratios for $^{13}C/^{12}C$, $^{18}O/^{16}O$, and D/H in interstellar environments vary significantly from the standard terrestrial abundances, and depend both on the isotope and location within the galaxy. The Galactic $^{13}C/^{12}C$ ratio ranges from 0.01 to 0.05 [7], and has been reported to be as high as 0.09 in some sources [8]. The $^{18}O/^{16}O$ ratio has been reported to be as low as 0.002 in the local ISM, and as high as 0.004 in the Galactic center [7]. The Galactic D/H ratio is 1.7×10^{-5} [7], though isotopic fractionation effects can raise the observed D/H ratio for many molecules by several orders of magnitude, as evidenced by the detection of ND_3 [9] in cold clouds. Given these abundances, it is expected that as more sensitive observatories such as ALMA come online, the isotopologues of glycolaldehyde may be observable toward some Galactic sources, particularly in the Galactic Center. Accurate transition frequencies for the various isotopic species of glycolaldehyde are therefore necessary to eliminate confusion between unassigned spectral features arising from known interstellar species and spectral features arising from truly unidentified species. Additionally, isotopic fractionation is strongly dependent on physical conditions present during formation, and determination of isotopic fractionation in glycolaldehyde may provide insight into the formation pathways for interstellar glycoladehyde.

The rotational spectrum of glycolaldehyde has been well-studied. The main glycolaldehyde isotopologue has been characterized

* Corresponding author. Fax: +1 434 924 3710 (B.H. Pate); Fax: +1 404 727 6586 (S.L. Widicus Weaver).
E-mail addresses: brookspate@virginia.edu, bp2k@virginia.edu (B.H. Pate), swidicu@emory.edu, susanna.widicus.weaver@emory.edu (S.L. Widicus Weaver).

0022-2852/$ - see front matter © 2013 Elsevier Inc. All rights reserved.
http://dx.doi.org/10.1016/j.jms.2013.01.002

to 1.2 THz [10–14]. The three singly-deuterated species have been studied from 12.3 to 26 GHz with J_{max} = 33 [10], and from 150 to 630 GHz with J_{max} = 67 [15]. The two ^{13}C isotopologues have been studied in the 12.3–26 GHz frequency range with J_{max} = 8 and J_{max} = 14 [11]. Spectral assignments for the two ^{13}C isotopologues from 150 to 945 GHz were also recently reported [17]. Additionally, $HC^{18}OCH_2OH$ has been studied from 12.4 to 36.3 GHz with J_{max} = 15 [11]. $HCOCH_2{}^{18}OH$ was not included in the previous microwave studies due to difficulties in isotopically-enriching the hydroxyl oxygen, and therefore has no reported microwave spectra. Sensitivity limitations with previous microwave spectral techniques led to only a handful of lines being measured at lower frequencies for each of these glycolaldehyde isotopic variants. These microwave measurements underpin the spectral predictions for higher frequency transitions that are applicable to new observational studies. It is therefore important to revisit these measurements with new high-sensitivity microwave spectrometers so that the spectral fits can be refined by inclusion of additional line assignments.

Here we report the laboratory rotational spectroscopic studies of the various glycolaldehyde isotopologues observed in natural abundance using pulsed-jet chirped pulse Fourier transform microwave spectrometers operating in the ranges of 6.5–20 GHz and 25–40 GHz. These measurements refine the previously reported measurements by offering higher spectral resolution, and improve upon the previous datasets with the inclusion of more transitions for each isotopologue. The experimental details, data analysis methods, and refined molecular parameters are presented below.

2. Experimental

Glycolaldehyde spectra were acquired at the University of Virginia, using two chirped-pulse Fourier transform microwave (CP-FTMW) spectrometers operating in the frequency ranges of 6.5–20 GHz and 25–40 GHz. The spectra are shown in Figs. 1–4. The 6.5–20 GHz spectrum was acquired using a CP-FTMW spectrometer that was previously described [18], and the 25–40 GHz spectrum was acquired using a newly-developed K_a band CP-FTMW spectrometer that has been recently described [19]. In both cases, a sample of 99% pure solid glycolaldehyde from Sigma–Aldrich was used without further purification or alteration. For both experiments, the sample was placed in a sample holder and gently heated to a temperature of 45 °C to produce sufficient gas-phase sample. Neon gas flowed over the solid sample, and the gas mixture was delivered to two pulsed valves (1 mm nozzle diameter, General Valve Series 9) at a backing pressure of ~1 atm. A total of 450 000 and 1 100 000 individual free induction decays (FIDs) were acquired for the low-frequency and high-frequency bands, respectively. A total of 10 FIDs were acquired on each valve cycle. The FID lengths were 20 μs and 10 μs in the low-frequency and high-frequency bands, respectively. These FIDs were averaged and converted to frequency spectra by taking a fast Fourier transform (FFT), and a Kaiser-Bessel window was applied. The resultant spectra given in Figs. 1–4 are magnitude spectra. The FWHM linewidths are on the order of 130 kHz in the low-frequency band and 200 kHz in the high-frequency band.

The strongest transition observed in the 6.5–20 GHz spectrum was the $1_{1,0}$–$1_{0,1}$ transition for $HCOCH_2OH$, with a signal strength

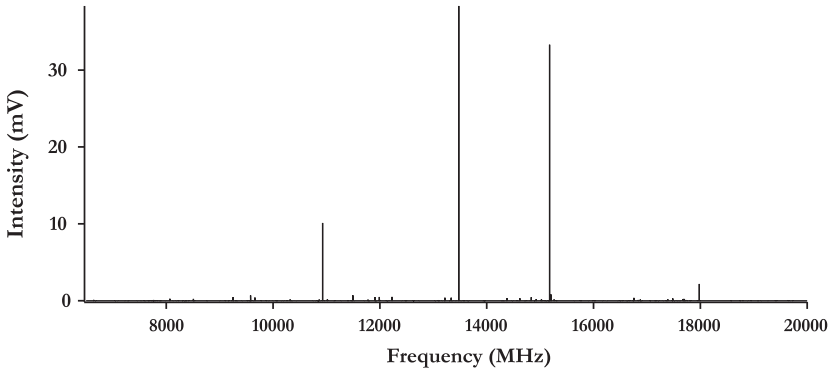

Fig. 1. Spectrum of glycolaldehyde from 6.5 to 20 GHz.

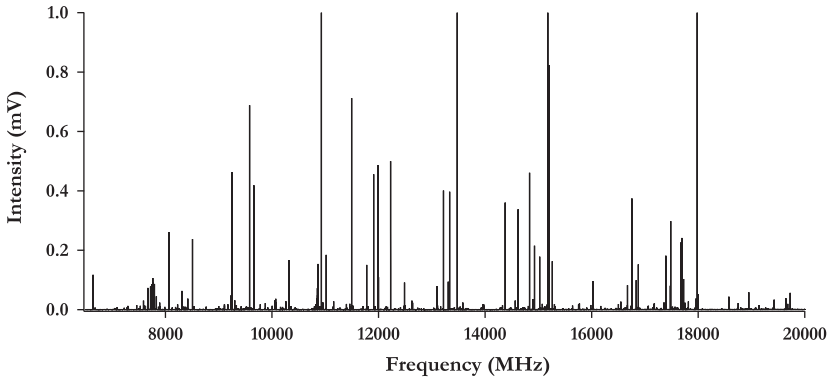

Fig. 2. Spectrum of glycolaldehyde from 6.5 to 20 GHz, showing spectral detail.

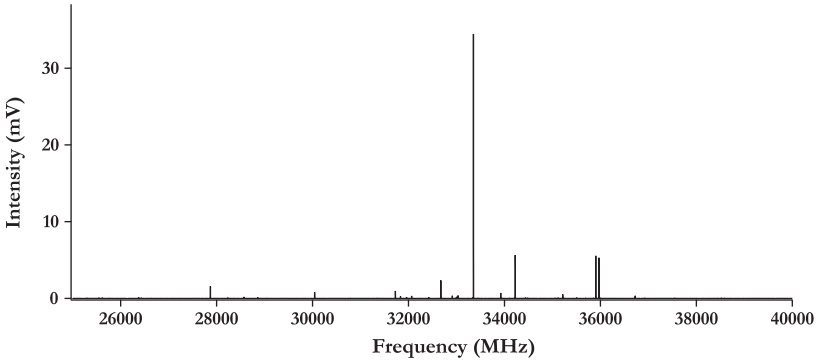

Fig. 3. Spectrum of glycolaldehyde from 25 to 40 GHz.

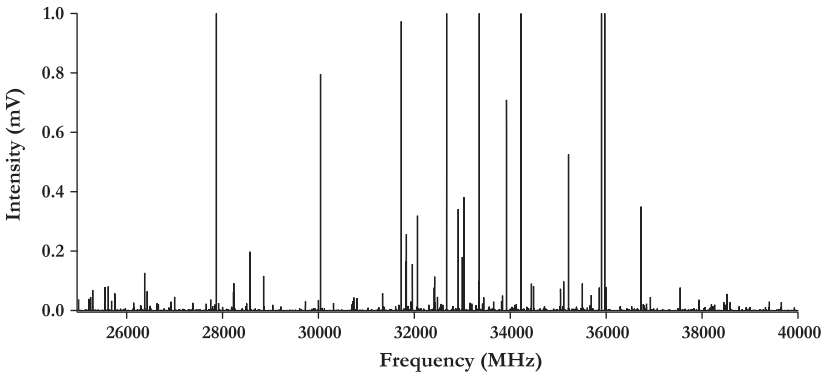

Fig. 4. Spectrum of glycolaldehyde from 25 to 40 GHz, showing spectral detail.

of 38.34 mV. The noise level in this spectrum is approximately 0.0003 mV,, based on an average of 450000 FIDs, giving a signal-to-noise ratio of ~127800 for the main isotopologue. In the 25–40 GHz spectrum, the strongest observed line was the $2_{1,2}$–$1_{0,1}$ transition for $HCOCH_2OH$, with a peak intensity of 34.45 mV. The noise level is approximately 0.00015 mV, based on an average of 1100000 FIDs, giving a signal-to-noise ratio of ~230000.

3. Data analysis

3.1. Initial fit parameters

The rotational constants and quartic centrifugal distortion constants for the singly deuterated species $DCOCH_2OH$, $HCOCDHOH$, and $HCOCH_2OD$ were taken from [15], and rotational constants for the ^{13}C isotopologues and $HCO^{18}CH_2OH$ were taken from [11]. Structural optimizations were performed for $HCOCH_2{}^{18}OH$ up to the B3LYP level of theory with an aug-cc-pVQZ basis set using GAUSSIAN 09 [20] at the Emory University Cherry L. Emerson Center for Scientific Computation. Single-point calculations were then performed on the minimum-energy geometry to determine equilibrium rotational constants and centrifugal distortion constants. The resulting constants were multiplied by the ratio of the experimentally-determined value for the main isotopologue [14] to its calculated value at the corresponding level of theory and basis set. This approach provided significantly more accurate constants without necessitating a rigorous treatment of contributions from zero-point energy and rovibrational interactions. This procedure was repeated for the singly-substituted ^{13}C isotopologues and $HCO^{18}CH_2OH$, giving excellent agreement with previously reported constants. Additionally, the rotational constants for the doubly-substituted ^{13}C and ^{18}O species and the two ^{17}O species were cal-

Table 1
Scaled theoretical rotational constants for glycolaldehyde isotopologues compared to previous experimental results.

Isotope	Calculated[a]			Experimentally determined[b]			% Difference		
	A (MHz)	*B* (MHz)	*C* (MHz)	*A* (MHz)	*B* (MHz)	*C* (MHz)	*A*	*B*	*C*
$H^{13}COCH_2OH$	18259.8	6474.5	4925.8	18259.524	6472.328	4924.556	−0.0262	0.0016	0.972
$HCO^{13}CH_2OH$	18139.9	6488.8	4925.5	18126.88	6487.47	4923.03	0.0759	−0.0337	0.982
$HC^{18}OCH_2OH$	18086.8	6241.5	4777.6	18087.032	6242.805	4778.491	0.0152	−0.0394	0.960
$HCOCH_2{}^{18}OH$	18087.8	6239.0	4776.2	N/A	N/A	N/A	N/A	N/A	N/A
$HC^{17}OCH_2OH$	18255.4	6381.0	4871.1	N/A	N/A	N/A	N/A	N/A	N/A
$HCOCH_2{}^{17}OH$	18255.8	6378.5	4869.7	N/A	N/A	N/A	N/A	N/A	N/A
$H^{13}CO^{13}CH_2OH$	17962.0	6434.7	4881.2	N/A	N/A	N/A	N/A	N/A	N/A
$HC^{18}OCH_2{}^{18}OH$	17717.0	5967.3	4590.6	N/A	N/A	N/A	N/A	N/A	N/A

[a] Gaussian output for a given constant at the B3LYP/aug-cc-pVQZ level of theory multiplied by the ratio of the corresponding experimentally-determined value to the calculated value for the main isotopologue.
[b] Taken from Refs. [10–14].

culated. The resulting rotational constants, adjusted for this scaling factor, are given in Table 1; all calculated constants given in subsequent Tables are the unscaled values. The dipole moment was assumed to be unchanged upon isotopic substitution, and the values determined for $HCOCH_2OH$ given in [11] of $\mu_a = 2.33$ D and $\mu_b = 0.262$ D were used for all isotopologues.

3.2. Spectral fitting and discussion

All spectral fitting was performed using the CALPGM program suite [21,22] using a standard asymmetric rotor Hamiltonian with a Watson A reduction in the I^r representation. Only rotational constants and quartic centrifugal distortion constants were included; higher order centrifugal distortion constants were found to have negligible impact on the quality of the fit. All uncertainties reported by SPFIT were converted to standard 1σ uncertainties using the PIFORM program [23]. Spectra showing the laboratory spectral detail compared to the simulations for each isotopologue are given in Fig. 5.

A total of 9, 4, and 7 new lines were assigned for $HCOCH_2OD$, $DCOCH_2OH$, and HCOCDHOH, respectively. The assigned transitions are given in Tables 2–4, respectively. Given the large number of assigned transitions in [15], no attempt was made to refine the constants determined in this work. Comparison of the measured frequencies in the current work with a prediction from the submillimeter study confirms that the assignments listed in Tables 2–4 are correct. It should be noted that the assignment for the $11_{4,6}$–$10_{5,5}$ transition at 24612.95 MHz listed in the previous study [16] has a typographical error in the quantum number assignment, as this transition is predicted to occur at 125.121 GHz. While it is likely that the correct assignment is the $11_{4,8}$–$10_{5,5}$ transition, which is predicted to lie at 24612.96 MHz, we have not included this assignment in our analysis.

Transitions for $H^{13}COCH_2OH$, $HCO^{13}CH_2OH$, and $HC^{18}OCH_2OH$ were assigned by starting with a data set and prediction based on the reported constants from previous work [16,11]. Transitions for all other isotopologues were assigned using predictions based on the calculated constants given in Table 1. In the case of transitions observed in both the current study and the original microwave studies, the value with the lower experimental uncertainty was used in the fit. The fit was rerun after each new line addition and a new spectral prediction was created. This process was performed iteratively until all transitions that could be observed for a given species were assigned. After initial fitting, it was noted that many transitions from previous work had an observed-minus-calculated residual that were much higher than their reported uncertainty, significantly increasing the RMS of the fit. These lines were removed from the fit, improving the RMS of the fit by several orders of magnitude.

A millimeter/submillimeter study of the ^{13}C-substituted glycolaldehyde species was accepted for publication during the preparation of this manuscript [17]. The results presented in the current study agree with the results from this higher-frequency work, and we have not attempted to refine the constants for $H^{13}COCH_2$-

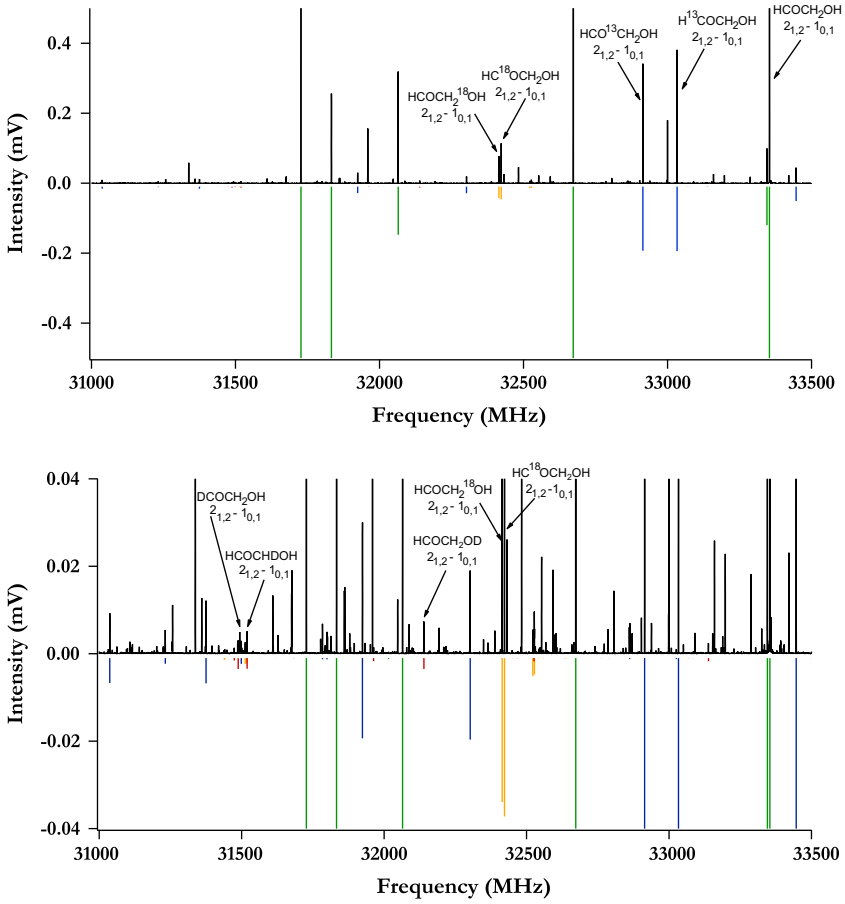

Fig. 5. Experimental spectra (black traces, positive spectra) compared to simulated stick spectra for each isotopologue (negative spectra), highlighting the assignments for the $2_{1,2}$–$1_{0,1}$ transition for each isotopologue. The simulation for the main isotopologue is scaled to match the experimental spectrum; the other isotopologues are scaled according to their natural abundance. The peak of the line from the main isotopologue is off-scale at 34.45 mV. A rotational temperature of 2 K was assumed for the simulations. The main isotopologue is shown in green, the ^{13}C isotopologues in blue, the ^{18}O isotopologues in yellow, and the D isotopologues in red.

Table 2
Newly assigned transitions and frequencies for $HCOCH_2OD$.

J'	K'_a	K'_c	J''	K''_a	K''_c	Observed frequency (MHz)	Marstokk and Møllendal [10] (MHz)	Obs. – Calc.[a] (MHz)	Uncertainty (MHz)
2	0	2	1	0	1	11608.6037	–	−0.0158	0.01
1	1	0	1	0	1	12607.7137	12607.77	0.0067	0.01
2	1	1	2	0	2	14390.0337	14390.33	0.0252	0.01
4	2	2	4	1	3	30036.8803	–	0.0179	0.02
3	2	1	3	1	2	31473.9423	–	0.0181	0.02
2	1	2	1	0	1	32139.5181	–	0.0028	0.02
2	2	0	2	1	1	33138.2800	–	−0.0141	0.02
4	0	4	3	1	3	36301.4585	–	−0.0074	0.02
2	2	1	2	1	2	37822.8550	–	0.0163	0.02

[a] Calculated values were predicted using the constants given in [15], and are compared to the experimentally determined values listed here.

Table 3
Newly assigned transitions and frequencies for $DCOCH_2OH$.

J'	K'_a	K'_c	J''	K''_a	K''_c	Observed frequency (MHz)	Marstokk and Møllendal [10] (MHz)	Obs. – Calc.[a] (MHz)	Uncertainty (MHz)
2	0	2	1	1	1	11333.3477	–	−0.0242	0.01
1	1	0	1	0	1	12372.0557	12372.23	0.0053	0.01
2	1	1	2	0	2	14117.9057	14118.04	0.0110	0.01
3	2	1	3	1	2	30894.2211	–	−0.0358	0.02
2	1	2	1	0	1	31487.7553	–	−0.0069	0.02
2	2	0	2	1	1	32526.1342	–	0.0443	0.02
4	0	4	3	1	3	35508.7387	–	−0.0196	0.02
2	2	1	2	1	2	37115.9259	–	0.0523	0.02

[a] Calculated values were predicted using the constants given in [15], and are compared to the experimentally determined values listed here.

Table 4
Newly assigned transitions and frequencies for HCOCHDOH.

J'	K'_a	K'_c	J''	K''_a	K''_c	Observed frequency (MHz)	Marstokk and Møllendal [10] (MHz)	Obs. – Calc.[a] (MHz)	Uncertainty (MHz)
2	0	2	1	1	1	11699.7437	–	−0.0040	0.01
1	1	0	1	0	1	12143.9437	–	−0.0214	0.01
2	1	1	2	0	2	13841.7037	13841.87	−0.0264	0.01
3	2	1	3	1	2	30368.5161	–	0.0074	0.02
2	1	2	1	0	1	31519.2138	–	−0.0076	0.02
2	2	0	2	1	1	31963.1344	–	0.0022	0.02
4	0	4	3	1	3	36015.7902	–	−0.0413	0.02
2	2	1	2	1	2	36431.6126	–	0.0014	0.02

[a] Calculated values were predicted using the constants given in [15], and are compared to the experimentally determined values listed here.

OH or $HCO^{13}CH_2OH$. A total of 24 transitions were observed for $H^{13}COCH_2OH$, of which 10 were new assignments. Five transitions from [11] appear to be bad assignments, based on their residuals. In particular, the $7_{2,5}$–$6_{3,4}$ transition at 27761.1200 MHz assigned in previous work [11] differs by more than 1 MHz from its predicted frequency. This is a weak transition, and there is no obvious match to this transition observed in the new spectrum. The assigned transitions for $H^{13}COCH_2OH$ are given in Table 5. These results agree well with the results from the recent millimeter/submillimeter study [17].

Initial attempts to assign the spectra of $HCO^{13}CH_2OH$ based on the information given in [11] were unsuccessful. The transitions reported in previous studies [11] can be fit using an asymmetric rotor Hamiltonian with the reported rotational constants quite well; however, the reported transitions are not observed in the spectra

Table 5
Newly assigned transitions and frequencies for $H^{13}COCH_2OH$.

J'	K'_a	K'_c	J''	K''_a	K''_c	Observed frequency (MHz)	Obs. – Calc.[a] (MHz)	Uncertainty (MHz)
2	2	0	3	1	3	8362.8457	−0.0147	0.01
2	0	2	1	1	1	10864.2611	−0.0071	0.01
1	0	1	0	0	0	11397.0121	−0.008	0.01
1	1	0	1	0	1	13334.7751	−0.0064	0.01
2	1	1	2	0	2	15025.2085	−0.0147	0.01
4	1	3	3	2	2	15237.3925	−0.0337	0.01
3	1	2	3	0	3	17815.7633	−0.0401	0.01
5	1	4	5	0	5	27660.1874	−0.0085	0.02
5	1	4	4	2	3	29898.4955	−0.0431	0.02
5	2	3	5	1	4	31374.8986	−0.0034	0.02
6	2	4	6	1	5	31498.6619	−0.0019	0.02
3	1	3	2	1	2	31783.7339	−0.0071	0.02
4	2	2	4	1	3	32302.0769	0.0015	0.02
7	2	5	7	1	6	33025.7012	−0.0110	0.02
2	1	2	1	0	1	33033.2407	0.00003	0.02
3	0	3	2	0	2	33627.8979	−0.0025	0.02
3	2	1	3	1	2	33838.4104	0.0033	0.02
3	2	2	2	2	1	34190.9735	0.0127	0.02
3	2	1	2	2	0	34753.5378	−0.0015	0.02
6	1	5	6	0	6	34967.4146	−0.0158	0.02
2	2	0	2	1	1	35503.3463	−0.0021	0.02
4	0	4	3	1	3	35690.2636	−0.0145	0.02
8	2	6	8	1	7	36222.4572	−0.0273	0.02
3	1	2	2	1	1	36418.4407	−0.0399	0.02

[a] Calculated values were predicted using the constants given in [17], and are compared to the experimentally determined values listed here.

Table 6
Newly assigned transitions and frequencies for $HCO^{13}CH_2OH$.

J'	K'_a	K'_c	J''	K''_a	K''_c	Observed frequency (MHz)	Obs. – Calc.[a] (MHz)	Uncertainty (MHz)
2	0	2	1	1	1	11017.8565	−0.0085	0.01
1	0	1	0	0	0	11410.3643	0.0084	0.01
1	1	0	1	0	1	13218.2831	−0.0070	0.01
2	1	1	2	0	2	14927.3526	−0.0114	0.01
4	1	3	3	2	2	15722.2993	−0.0461	0.01
3	1	2	3	0	3	17752.8143	−0.0359	0.01
5	1	4	5	0	5	27730.6992	−0.0183	0.02
6	2	4	6	1	5	31231.8823	−0.0110	0.02
3	1	3	2	1	2	31799.6146	−0.0095	0.02
4	2	2	4	1	3	31924.0947	0.0042	0.02
2	1	2	1	0	1	32914.4125	−0.0045	0.02
3	2	1	3	1	2	33446.4473	0.0003	0.02
3	0	3	2	0	2	33652.0145	−0.0104	0.02
3	2	2	2	2	1	34230.9783	−0.0249	0.02
3	2	1	2	2	0	34809.5220	0.0055	0.02
2	2	0	2	1	1	35114.4440	0.0024	0.02
6	1	5	6	0	6	35126.8776	−0.0048	0.02
4	0	4	3	1	3	35856.6028	−0.0065	0.02
3	1	2	2	1	1	36477.5053	−0.0058	0.02
2	2	1	2	1	2	39654.4929	−0.0114	0.02

[a] Calculated values were predicted using the constants given in [17], and are compared to the experimentally determined values listed here.

from the current study. In the original study, it was noted that observation of the ^{13}C species in natural abundance was extremely difficult, with only very weak b-type transitions being observed. The B rotational constant in the previous study was not explicitly calculated, but generated by taking plausible values at 3 MHz intervals. It is possible that this method, combined with the low signal-to-noise ratio available in this work, led to an incorrect assignment of the $HCO^{13}CH_2OH$ spectrum. However, it is difficult to determine if this is in fact the cause of the discrepancy without performing a reanalysis of the original dataset. We have therefore assigned the transitions for $HCO^{13}CH_2OH$ reported here based on

Table 7
All assigned transitions and frequencies for $HC^{18}OCH_2OH$ based on current and previous studies.

J'	K'_a	K'_c	J''	K''_a	K''_c	Observed frequency (MHz)	Obs. – Calc. (MHz)	Uncertainty (MHz)
2	0	2	1	1	1	10070.6227	−0.0089	0.01
1	0	1	0	0	0	11021.2899	0.0129	0.01
1	1	0	1	0	1	13308.5290	0.0005	0.01
2	1	1	2	0	2	14900.3580	−0.0125	0.01
3	0	3	2	1	2	22051.8700	−0.0069	0.10
1	1	1	0	0	0	22865.5200	−0.0007	0.10
5	1	4	5	0	5	26717.3894	−0.0001	0.02
11	7	5	12	6	6	28995.1100	−0.0876	0.10
11	7	4	12	6	7	29004.0800	−0.0763	0.10
3	1	3	2	1	2	30790.6679	0.0021	0.02
6	2	4	6	1	5	31439.2355	0.0171	0.02
5	2	3	5	1	4	31512.5661	−0.0205	0.02
13	8	5	14	7	8	31719.7500	0.0175	0.10
2	1	2	1	0	1	32422.5312	0.0100	0.02
4	2	2	4	1	3	32521.8211	−0.0079	0.02
3	0	3	2	0	2	32559.4830	−0.0281	0.02
6	1	5	6	0	6	33570.2329	−0.0042	0.02
13	4	10	12	5	7	34035.2900	0.0304	0.02
3	2	1	3	1	2	34051.3958	0.0026	0.02
4	0	4	3	1	3	34124.1887	−0.0231	0.02
15	5	10	14	6	9	34830.3300	−0.0002	0.10
3	1	2	2	1	1	35176.2241	0.0438	0.02
2	2	0	2	1	1	35660.0465	0.0109	0.02
2	2	1	2	1	2	39925.2456	0.0040	0.02

Table 8
Experimentally determined rotational constants for $HC^{18}OCH_2OH$ based on the combined dataset given in Table 7, compared to results from previous experiments and theory.

Parameter	Value (Uncertainty)	Marstokk and Møllendal [16]	B3LYP/aug-cc-pVQZ	Units
A	18087.0469(48)	18087.032(26)	18259.07	MHz
B	6242.8120(18)	6242.805(9)	6232.20	MHz
C	4778.4877(20)	4778.491(12)	4783.21	MHz
Δ_J	5.698(30)		6.03	kHz
Δ_{JK}	−20.05(27)		−21.7	kHz
Δ_K	45.24(14)		49.6	kHz
δ_J	1.728(23)		1.75	kHz
δ_K	9.35(52)		8.29	kHz
Fit RMS	28.5			kHz
Lines	24			

Table 9
Assigned transitions and frequencies for $HCOCH_2{}^{18}OH$.

J'	K'_a	K'_c	J''	K''_a	K''_c	Observed frequency (MHz)	Obs. – Calc. (MHz)	Uncertainty (MHz)
2	0	2	1	1	1	10058.0662	−0.0070	0.01
1	0	1	0	0	0	11015.7294	−0.0018	0.01
1	1	0	1	0	1	13308.8910	0.0012	0.01
2	1	1	2	0	2	14899.1443	−0.0034	0.01
5	1	4	4	2	3	27420.7623	−0.0031	0.02
3	1	3	2	1	2	30776.1711	0.0021	0.02
6	2	4	6	1	5	31440.5067	0.0015	0.02
5	2	3	5	1	4	31517.1106	−0.0004	0.02
2	1	2	1	0	1	32414.4769	−0.0001	0.02
3	0	3	2	0	2	32543.8150	0.0110	0.02
6	1	5	6	0	6	33548.5219	0.0011	0.02
3	2	1	3	1	2	34057.1566	−0.0069	0.02
4	0	4	3	1	3	34100.1949	0.0058	0.02
3	1	2	2	1	1	35157.6682	−0.0103	0.02
2	2	0	2	1	1	35664.8907	−0.0033	0.02
2	2	1	2	1	2	39926.3192	0.0060	0.02

Table 10
Experimentally determined rotational constants for $HCOCH_2{}^{18}OH$ compared to results from theory.

Parameter	Value (Uncertainty)	B3LYP/aug-cc-pVQZ	Units
A	18085.3081(46)	18260.16	MHz
B	6239.3692(21)	6229.69	MHz
C	4776.3858(30)	4781.78	MHz
Δ_J	5.936(34)	6.02	kHz
Δ_{JK}	−21.01(42)	−21.1	kHz
Δ_K	47.3(10)	49.2	kHz
δ_J	1.686(16)	1.74	kHz
δ_K	10.30(89)	8.52	kHz
Fit RMS	5.2		kHz
Lines	16		

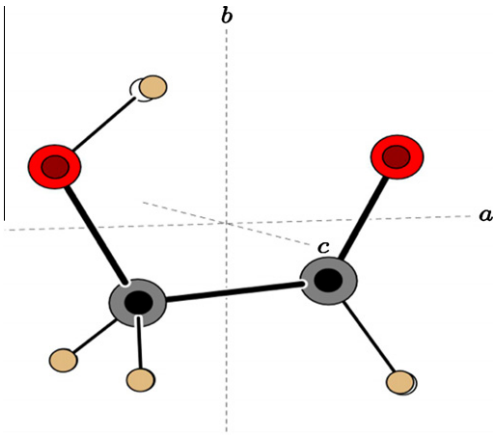

Fig. 6. Kraitchman structure of glycolaldehyde. The darker spheres denote the experimentally-determined atom positions, and the lighter spheres denote the calculated atom positions determined at the MP2/6-311++G (d,p) level of theory.

the theoretically calculated rotational constants given in Table 1. The assigned transitions for $HCOC^{13}H_2OH$ are given in Table 6. These assignments agree well with the results from the recent millimeter/submillimeter study [17].

A total of 22 transitions were assigned for $HC^{18}OCH_2OH$, of which 8 were new assignments. Six previously reported transitions were removed from the list of assignments. The final fit had a microwave RMS of 28.5 kHz. The assigned transitions for $HC^{18}OCH_2OH$ are given in Table 7, and the final fit parameters, previously derived parameters, and unscaled theoretical values are given in Table 8. Likewise, 16 transitions were assigned for $HCOCH_2{}^{18}OH$, giving a microwave RMS of 6.2 kHz. The assigned transitions for $HCOCH_2{}^{18}OH$ are given in Table 9, and the final fit parameters and unscaled theoretical values are given in Table 10.

A Kraitchman analysis was performed using the experimental rotational constants. The values for the ^{13}C and ^{18}O species determined in this work and the literature values for the main isotopologue [14] and the deuterium-substituted isotopologues [15] were used for this analysis. The resulting structure is shown in Fig. 6, the corresponding structural parameters are given in Table 11, and the Kraitchman coordinates are given in Table 12. These coordinates agree well with both the previously reported values and the theoretical values. There is, however, one discrepancy between experiment and theory. The Kraitchman analysis shows a significant deviation of the OH hydrogen position from that predicted by theory. This could be because theory inaccurately treats the intramolecular forces, or it could be that the substitution of the D-atom in a weak hydrogen bond violates the assumptions of the Kraitchman analysis. It would be expected that a non-dispersion corrected

Table 11
Comparison of experimentally determined structural parameters to those calculated at different levels of theory. Uncertainties are Costain errors.

Bond (Å)	This work	Marstokk and Møllendal [11]	MP2/6-311++G (d,p)	M062X/6-311++G (d,p)	B3LYP/6-311++G (d,p)	B3LYP/aug-cc-pVQZ
C═O	1.2102(36)	1.2094(3)	1.2164	1.2017	1.2079	1.2048
C—O	1.3996(32)	1.4366(7)	1.4030	1.3941	1.4015	1.3983
C—C	1.5012(29)	1.4987(4)	1.5097	1.5063	1.5070	1.5034
O—H	1.0554(29)	1.0510(5)	0.9669	0.9663	0.9692	0.9678
C—$H_{aldehyde}$	1.1038(27)	1.1021(3)	1.1059	1.1051	1.1076	1.1053
C—H	1.1030(20)	1.0930(3)	1.0994	1.0988	1.1011	1.0988
O···H	2.0011(30)	2.0069(4)	2.1036	2.1166	2.1403	2.1312
O···O	2.6851(15)	2.6974(4)	2.6980	2.6823	2.7060	2.6977
Angle (°)[a]						
C—C═O	121.90(43)	122.44(2)	121.94	121.83	122.14	122.19
C—C—$H_{aldehyde}$	115.97(35)	115.16(2)	116.44	116.67	116.28	116.21
C—C—O	112.28(31)	111.28(2)	112.26	112.29	112.80	112.66
C—O—H	102.35(32)	101.34(2)	105.50	107.23	106.92	106.89
C—C—H	108.37(29)	109.13(1)	107.64	107.72	107.77	107.79
H—C—H	106.18(28)	107.34(2)	107.24	106.87	106.41	106.21
H—C—O	110.69(34)	109.39(1)	110.93	111.00	110.91	111.05
O—H···O	119.67(33)	120.33(2)	118.15	115.81	115.75	115.85
H···O═C	83.78(23)	83.41(1)	82.14	82.852	82.39	82.40

Table 12
Experimentally-determined glycolaldehyde Kraitchman coordinates compared to those derived from ab initio calculations. The coordinates are planar except where noted. Bold characters denote the atom coordinate. Uncertainties are given as Costain errors.

Atom	$\|a\|$/Å	$\|b\|$/Å	$\|c\|$/Å
Experimental coordinates			
CH_2OHCHO	0.6902(22)	0.6854(22)	[0]
CH_2OH**C**HO	0.8037(19)	0.5366(28)	[0]
CH_2OHCH**O**	1.3387(11)	0.5486(27)	[0]
CH_2**O**HCHO	1.3467(11)	0.5507(27)	[0]
HOCH_2C**H**O	0.5420(28)	1.2337(12)	[0]
HOCH**H**CHO[a]	0.9803(15)	1.2809(12)	0.8820(17)
HOCH_2CHO	1.3832(11)	1.4761(10)	[0]
Theoretical coordinates calculated at MP2/6-311++G (d,p)			
CH_2OHCHO	−0.6970	−0.6881	0
CH_2OH**C**HO	0.8056	−0.5419	0
CH_2OHCH**O**	1.3462	0.5478	0
CH_2**O**HCHO	−1.3518	0.5527	0
HOCH_2C**H**O	−0.6484	1.2162	0
HOCH**H**CHO[a]	−0.9740	−1.2783	−0.8852
HOCH_2CHO	1.3916	−1.4798	0

[a] Nonplanar coordinates, second hydrogen position obtained by sign change.

method (like B3LYP) might noticeably vary from a dispersion corrected method (like M062X) or an MP2 type calculation. To test this, we computed the structure using M062X, MP2 and B3LYP methods using a 6-311++G (d,p) basis set. The results are given in Table 11, and show that all theoretical calculations performed during this work are consistent on the position of the OH hydrogen position. This can be explained if the standard assumption that isotopic substitution does not affect the nuclear coordinate is not valid for deuterium in a weak hydrogen bond. Furthermore, the results show that while DFT methods provide reasonable accuracy for modest computational time, MP2 more faithfully reproduces the structure. This is likely because MP2 methods more accurately account for long range interactions, even when compared with B3LYP using a higher basis set, as demonstrated by the O—H···O bond angle.

Given the long integration times used in this study, the signal-to-noise ratio achieved should be high enough to observe the strongest transitions from $H^{13}CO^{13}CH_2OH$, $HC^{17}OCH_2OH$, and $HCOCH_2{}^{17}OH$ species. While this is likely the case, an insufficient number of transitions were observed for these species to make a definitive assignment or determine molecular constants.

Table 13
Newly assigned transitions and frequencies for $HCOCH_2OH$.

J'	K'_a	K'_c	J''	K''_a	K''_c	Observed frequency (MHz)	Uncertainty (MHz)
4	3	1	5	2	4	6851.1874	0.01
6	4	2	7	3	5	7288.0255	0.01
8	1	8	7	2	5	8438.9934	0.01
2	2	0	3	1	3	8508.4981	0.01
10	2	8	11	1	11	9217.7297	0.01
3	1	2	3	1	3	9331.6062	0.01
1	0	1	0	0	0	11495.2044	0.01
4	1	3	3	2	2	15261.4104	0.01
4	1	3	4	1	4	15508.5052	0.01
3	3	1	4	2	2	15642.5810	0.01
3	3	0	4	2	3	17716.1675	0.01
9	2	8	8	3	5	27291.5117	0.02
7	2	5	6	3	4	27793.0905	0.02
5	1	4	4	2	3	30043.1021	0.02
4	4	1	5	3	2	30536.8258	0.02
4	4	0	5	3	3	30764.0284	0.02
10	2	9	9	3	6	31506.4600	0.02
3	1	3	2	1	2	32064.8337	0.02
3	0	3	2	0	2	33922.0167	0.02
3	2	1	2	2	0	35048.5211	0.02
3	1	2	2	1	1	36726.3943	0.02

Finally, several previously unobserved lines were assigned for the main isotopologue ($HCOCH_2OH$). These transitions were assigned based on the constants reported in [14], but no attempt was made to refine the fit. The newly-assigned transitions are listed in Table 13.

4. Conclusion

We have acquired and assigned the rotational spectrum of glycolaldehyde in two spectral windows, 6.5–20 GHz and 25–40 GHz. Transitions arising from the isotopologues of glycolaldehyde in natural abundance have been assigned based on previously reported data and ab initio calculations. Fitting of the observed transitions to an asymmetric top Hamiltonian with a small set of parameters gives microwave RMS values near the experimental uncertainty.

The molecular parameters for the glycolaldehyde isotopologues have been significantly refined based on the new spectral information gained through this study. The assignment of the glycolaldehyde isotopic species was relatively straightforward, in particular for those species with previously reported transitions and rota-

tional constants. The low temperatures achieved in the supersonic expansion source greatly simplified the spectra, and the deep signal averaging enabled the assignment of previously unobserved transitions. These transitions were readily combined with previously reported transitions to give a single data set that gave an excellent fit using a standard asymmetric rotor Hamiltonian. The rotational constants calculated for each molecule also proved to be extremely accurate, and allowed for a rapid reassignment of each species based solely on these constants as a check of previously reported rotational constants. Finally, a Kraitchman analysis was performed using the experimental rotational constants to determine the molecular structure of glycolaldehyde.

The information provided from this work can be used to guide higher-frequency studies that are directly applicable to observations of glycolaldehyde isotopologues in star-forming regions. Additionally, this work demonstrates the utility of rapid acquisition, high-sensitivity spectral techniques for the study of astrophysically-important molecules.

Acknowledgments

This work was supported by the Centers for Chemical Innovation program of the National Science Foundation (CHE-0847919) and SLWW's startup funding from Emory University. The computational studies were supported by an NSF MRI-R2 Grant (CHE-0958205) and utilized the resources of the Cherry Emerson Center for Scientific Computation.

References

[1] J.M. Hollis, F.J. Lovas, P.R. Jewell, Astrophys. J. Lett. 540 (2000) L107–L110.
[2] J.M. Hollis, S.N. Vogel, L.E. Snyder, P.R. Jewell, F.J. Lovas, Astrophys. J. Lett. 554 (2002) L81–L85.
[3] D.T. Halfen, A.J. Apponi, N. Woolf, R. Polt, L.M. Ziurys, Astrophys. J. 639 (2006) 237–245.
[4] M.T. Beltrán, C. Codella, S. Viti, R. Neri, R. Cesaroni, Astrophys. J. Lett. 690 (2009) L93–L96.
[5] J.K. Jørgensen, C. Favre, S.E. Bisschop, T.L. Bourke, E.F. van Dishoeck, M. Schmalzl, Astrophys. J. Lett. 757 (2012) L4–L8.
[6] M.T. Beltrán, R. Cesaroni, R. Neri, C. Codella, R.S. Furuya, S. Viti, L. Testi, L. Olmi, Astron. Astrophys. 435 (2005) 901–925.
[7] T.L. Wilson, R.T. Rood, Annu. Rev. Astron. Astrophys. 32 (1994) 191–226.
[8] J.G. Mangum, R.T. Rood, E.J. Wadiak, T.L. Wilson, ApJ 334 (1988) 182–190.
[9] D.C. Lis, E. Roueff, M. Gerin, T.G. Phillips, L.H. Coudert, F.F.S. van der Tak, P. Schilke, Astrophys. J. Lett. 571 (2002) L55–58.
[10] K.M. Marstokk, H. Møllendal, J. Mol. Struct. 5 (1970) 205–213.
[11] K.M. Marstokk, H. Møllendal, J. Mol. Struct. 16 (1973) 259–270.
[12] R.A.H. Butler, F.C. De Lucia, D.T. Petkie, H. Møllendal, A. Horn, E. Herbst, Astrophys. J. 134 (2001) 319–321.
[13] S.L. Widicus Weaver, R.A.H. Butler, B.J. Drouin, D.T. Petkie, K.A. Dyl, F.C. De Lucia, G.A. Blake, Astrophys. J. Supple. 158 (2005) 188–192.
[14] P.B. Carroll, B.J. Drouin, S.L. Widicus Weaver, ApJ 723 (2010) 845–849.
[15] A. Bouchez, L. Margulés, R.A. Motiyenko, J-C. Guillemin, A. Walters, S. Bottinelli, C. Ceccarelli, C. Kahane, Astron. Astrophys. 540 (2012) A51.
[16] K.M. Marstokk, H. Møllendal, J. Mol. Struct. 7 (1971) 101–109.
[17] I. Haykal, R.A. Motiyenko, L. Margulés, T.R. Huet, Astron. Astrophys. (2012).
[18] G.G. Brown, B.C. Dian, K.O. Douglas, S.M. Geyer, S.T. Shipman, B.H. Pate, Rev. Sci. Inst. 79 (2008) 053103-1–053103-13.
[19] D.P. Zaleski, J.L. Neill, M.T. Muckle, N.A. Seifert, P.B. Carroll, S.L. Widicus Weaver, B.H. Pate, J. Mol. Spectrosc. 280 (2012) 68–76.
[20] M.J. Frisch, G.W. Trucks, H.B. Schlegel, G.E. Scuseria, M.A. Robb, J.R. Cheeseman, G. Scalmani, V. Barone, B. Mennucci, G.A. Petersson, H. Nakatsuji, M. Caricato, X. Li, H.P. Hratchian, A.F. Izmaylov, J. Bloino, G. Zheng, J.L. Sonnenberg, M. Hada, M. Ehara, K. Toyota, R. Fukuda, J. Hasegawa, M. Ishida, T. Nakajima, Y. Honda, O. Kitao, H. Nakai, T. Vreven, J.A. Montgomery Jr., J.E. Peralta, F. Ogliaro, M. Bearpark, J.J. Heyd, E. Brothers, K.N. Kudin, V.N. Staroverov, R. Kobayashi, J. Normand, K. Raghavachari, A. Rendell, J.C. Burant, S.S. Iyengar, J. Tomasi, M. Cossi, N. Rega, J.M. Millam, M. Klene, J.E. Knox, J.B. Cross, V. Bakken, C. Adamo, J. Jaramillo, R. Gomperts, R.E. Stratmann, O. Yazyev, A.J. Austin, R. Cammi, C. Pomelli, J.W. Ochterski, R.L. Martin, K. Morokuma, V.G. Zakrzewski, G.A. Voth, P. Salvador, J.J. Dannenberg, S. Dapprich, A.D. Daniels, O. Farkas, J.B. Foresman, J.V. Ortiz, J. Cioslowski, D.J. Fox, Gaussian, Inc., Wallingford CT, 2009.
[21] H.M. Pickett, J. Mol. Spectrosc. 148 (1991) 371–377.
[22] H.M. Pickett, SPFIT/SPCAT Package. <http://www.spec.jpl.nasa.gov>.
[23] Z. Kisiel, PIFORM. <http://www.ifpan.edu.pl/kisiel/asym/asym.htm#piform>.